

Passivity-based adaptive current control loop of cascaded H-bridge multilevel converter for grid-tied photovoltaic system

Tran Hung Cuong¹, An Thi Hoai Thu Anh²

¹Faculty of Electrical and Electronics Engineering, Thuyloi University, Hanoi, Vietnam

²Department of Electrical Engineering, University of Transport and Communications, Hanoi, Vietnam

Article Info

Article history:

Received Dec 8, 2023

Revised Oct 26, 2023

Accepted May 12, 2024

Keywords:

Cascaded H-bridge converter

Grid connection inverter

Multi-level converter

Passivity-based control

Photovoltaics power

ABSTRACT

This paper proposes an algorithm to passivity-based control (PBC) for the current control loop of the cascaded H-bridge converter (CHB) connecting the grid-connected PV system with the space vector modulation (SVM) algorithm using the law of expanding any number of voltage levels. The algorithm SVM in this paper is suitable for CHB converters. It can create a number of high levels of alternating voltage that other methods cannot do. Passivity-based control (PBC) algorithm aims to create a flexible controller that can change its structure or parameters to adapt to changes in the system, ensuring stable system quality, reducing switching losses and gaining energy conversion efficiency. It enhances the capability of accurately delivering power on demand to the grid with the CHB inverter in situations in which the grid demands the mobilization of maximum power from the photovoltaics (PV) system. The simulation results of the 9-level CHB system performed by MATLAB/Simulink software have proved the feasibility of the proposed algorithm.

This is an open access article under the [CC BY-SA](https://creativecommons.org/licenses/by-sa/4.0/) license.



Corresponding Author:

An Thi Hoai Thu Anh

Department of Electrical Engineering, Faculty of Electrical-Electronic Engineering, University of Transport and Communications

N0 3 Cau Giay, Lang Thuong Commune, Dong Da District, Hanoi, Vietnam

Email: htanh.ktd@utc.edu.vn

1. INTRODUCTION

Among various renewable energies, solar energy is a type of energy source that can be generated on a large scale and integrated with other renewable sources [1]–[7]. Therefore, grid-connected photovoltaics (PV) configurations always pay great attention and develop [8], [9]. The multi-level converter is one of the best converters to be chosen to connect the PV system to the grid at high voltage level. Despite the advantages offered by topologies like neutral point-clamped (NPC) and flying capacitor (FC) [10], the cascaded H-bridge (CHB) converter is of special interest because it is one of the feasible choices for large-scale solar energy conversion with numerous outstanding advantages such as having fewer components compared to converters at the same voltage level [10]–[13]; suitable for high-power, medium-voltage applications [8], [12], [14]; a modular structure and high reliability for easy voltage level adjustment and maintenance [15]. Thanks to these advantages, many applications have been implemented for CHB, such as a 13-level 7.2 kV CHB-based electric drive system [14] and static synchronous compensators (STATCOM) [15]. However, as the number of levels in CHB increases, the control of switching operations becomes much more stringent compared to conventional converters, so it is necessary to design optimal switching algorithms. To achieve this, it is necessary to have appropriate modulation and control algorithms to bring high efficiency in the power conversion process and ensuring that the output parameters of converter meet design requirements such as current, sinusoidal voltage, and total harmonic distortion within permissible limits.

Recently, there have been various control studies for grid-connected PV applications using CHB, including phase shift carrier based pulse width modulation (PSC-PWM); and level shift carrier based pulse width modulation (LS-PWM) [16]–[19]. Each modulation method has its advantages and disadvantages, but the main obstacle to modulation design is the number of CHB modules to increase [20]. To overcome this, this article proposes a space vector modulation (SVM) modulation algorithm with a law of expanding any number of voltage levels to easily implement the algorithm when increasing the number of levels of a modular multilevel converter (MMC). This method has smooth switching and low switching loss and is very suitable for CHBs with many levels. In a grid-connected multi-level CHB converter, inductors (L) and resistors (R) are indispensable for generating voltage differentials to transfer power from PV sources to the utility. However, in practice, the values of L and R can change with variations in ambient temperature, leading to errors that affect control algorithms and negatively impact the quality of current and voltage. To address the above problems, this paper proposes a passivity-based control algorithm that aims to adjust the values of the parameters R and L when affected by conditions outside the system to avoid disturbances arising during the energy conversion process. The core of this method is to utilize a linear control approach designed based on the linearized model at the working point. When the object transitions to a different working point in which the linear controller is not updated or parameters are not changed, there is a potential risk of degrading control quality [13], [21]. Therefore, this algorithm updates the necessary parameters R , L to ensure the requirements of power and electricity quality when the grid operates heavily. In this case, the main objective of this control algorithm is to make the AC current and voltage waveform sinusoidal with a low total harmonic distortion (THD) index below 5%. This algorithm can overcome the shortcomings when the grid operates in a heavy-duty mode, which proportional-integral (PI) control methods [22] cannot achieve. Simulation results are implemented in MATLAB/Simulink. Section 2, details the structure and mathematical model of the CHB converter are detailed. Section 3 is devoted to designing a passivity-based adaptive current control loop for the grid-connected CHB converter. Section 4 presents the simulation result of the proposed control strategy. The simulation objectives for the control algorithm are shown as the standard sinusoidal current and voltage, the power according to the desired reference value, and the capacitors operating stably in the allowed state.

2. CIRCUIT STRUCTURE AND MATHEMATICAL MODEL OF CHB CONVERTER

Figure 1 is the structure diagram of a 9-level CHB converter. Each H-bridge includes 4 insulated-gate bipolar transistor (IGBT) semiconductor switches, supplied by an independent DC source generated by PV panels and can produce three levels of output voltage: $+V_{DC}$, 0 , $-V_{DC}$ by switching the pairs of valves (S_1, S_2) và (S_3, S_4) [3], [23]. Equation (1) describes the AC side voltage of the CHB converter in Figure 1.

$$v_j = L \frac{di_j}{dt} + Ri_j \quad j = A, B, C \quad (1)$$

Assuming the three-phase load on the AC side is balanced, the voltage on each phase of the AC side:

$$\begin{cases} v_A = v_{AO} = v_{AN} + v_{NO} \\ v_B = v_{BO} = v_{BN} + v_{NO} \\ v_C = v_{CO} = v_{CN} + v_{NO} \end{cases} \quad (2)$$

Voltage v_{NO} is the common mode voltage with the value calculated in the (3).

$$v_{NO} = \frac{1}{3}[v_A + v_B + v_C] \quad (3)$$

Therefore:

$$v_j = \left[L \frac{di_j}{dt} + R \cdot i_j + v_{sj} \right] + v_{NO} \quad (4)$$

From (4) the relationship between converter current and voltage is described by (5):

$$\frac{di_j}{dt} = -\frac{R}{L} i_j + \frac{1}{L} [v_j - v_{NO} - v_{sj}] \quad (5)$$

Each voltage v_A, v_B, v_C can take one of three voltage levels $V_{DC}^* (-1, 0, 1)$ and is referred to as voltage state levels. From there we can write: $v_j = V_{DC} \cdot v_{lj}$ In there:

$$v_{lj} \in \{-1,0,1\} \tag{6}$$

To generate control signals, the output voltage is in the state space model on the $\alpha\beta$ coordinate system and is used (7).

$$V = \frac{2}{3}(v_{AN} + a \cdot v_{BN} + a^2 \cdot v_{CN}) \tag{7}$$

where:

$$\begin{cases} v_{AN} = k_A \cdot V_{DC} \\ v_{BN} = k_B \cdot V_{DC}; a = e^{j\frac{2\pi}{3}}; a^2 = e^{j\frac{4\pi}{3}}; \text{ with } k_A, k_B, k_C \in \left\{-\frac{M-1}{2}, \dots, -1, 0, 1, \dots, \frac{M-1}{2}\right\} \\ v_{CN} = k_C \cdot V_{DC} \end{cases}$$

when using this conversion (1) is described as (8):

$$L \frac{di_{\alpha,\beta}}{dt} + Ri_{\alpha,\beta} = v_{\alpha,\beta} \tag{8}$$

where $v_{\alpha\beta}$ are the voltage vectors and $i_{\alpha\beta}$ is the current vector on the AC side of the converter.

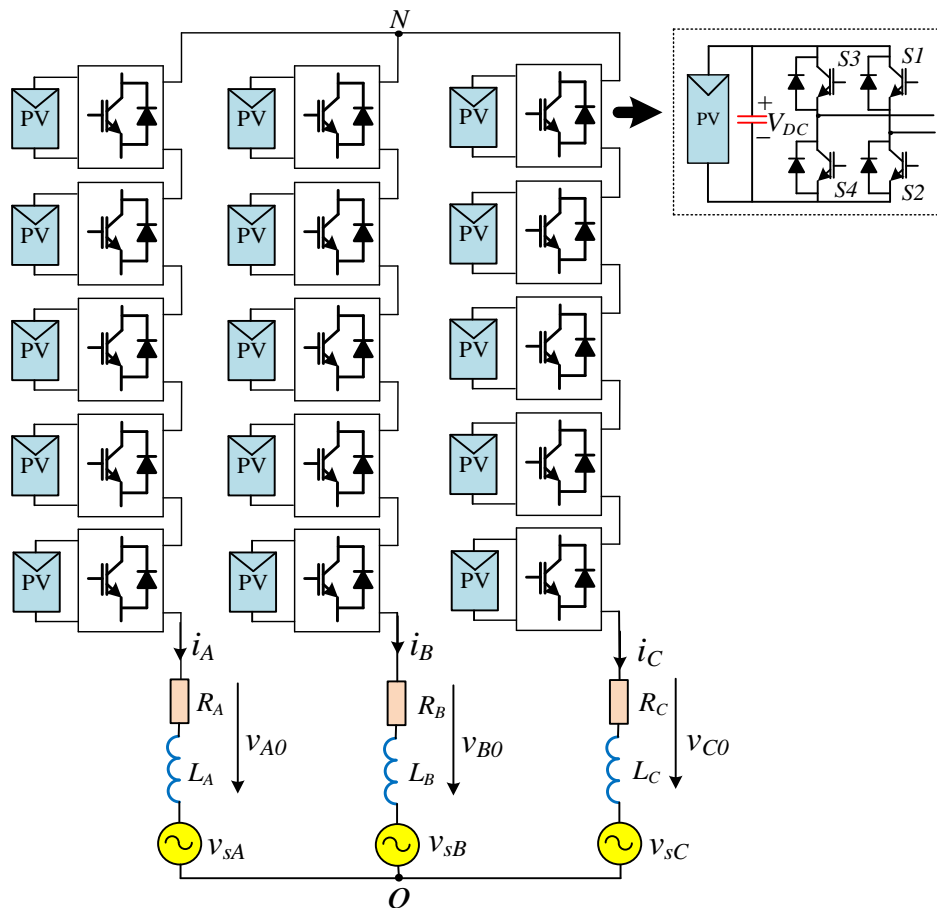


Figure 1. Structural diagram of a CHB converter connected to the grid

3. DESIGN PASSIVITY-BASED ADAPTIVE CURRENT CONTROL LOOP FOR THE GRID-CONNECTED CHB CONVERTER

Designing control for connecting the CHB converter to the grid includes two loop circuits: an inner current control loop and an outer voltage control loop [8], [11], with the current loop having a wide enough

bandwidth for the fastest possible response [12]. The control design is carried out in the dq coordinate system, with independent control of the d -axis and q -axis components through a passivity-based adaptive current control loop satisfying requirements to minimize steady-state error while achieving rapid response, reducing control signal chattering, and maintaining the desired sinusoidal current waveform [24]. The theory of the passivity-based algorithm is presented in [21], [24]. The passive system is based on energy conservation principles, meaning it does not generate energy independently [23], [25]. Passivity-based control (PBC) is a control algorithm whose principle is based on the passive characteristics of the system (open-loop) to make the closed-loop system a passive system with a desired energy storage function [16]. Adaptive control is adjusting a control system by observing its response [26]. This type of control is often proposed for systems with imprecisely determined parameters or these parameters are changed while operating. Adaptive control aims to create a flexible controller that can change its structure or parameters to adapt to changes in the system, ensuring stable system quality [26]. The mathematical model of BBDC represents:

$$\begin{cases} v_A = v_{sA} + R_A i_A + L_A \frac{di_A}{dt} \\ v_B = v_{sB} + R_B i_B + L_B \frac{di_B}{dt} \\ v_C = v_{sC} + R_C i_C + L_C \frac{di_C}{dt} \end{cases} \quad (9)$$

Equation (9) is rewritten on the dq coordinate to control the MMC easily, using the PARK coordinate displacement as (10).

$$\begin{cases} \frac{di_d}{dt} = -\frac{R}{L} i_d + \omega i_q + \frac{1}{L} (v_d - v_{sd}) \\ \frac{di_q}{dt} = -\frac{R}{L} i_q - \omega i_d + \frac{1}{L} (v_q - v_{sq}) \end{cases} \quad (10)$$

In this context, the linear control model with uncertain parameters is considered a nonlinear system, and a positive definite function $V(e)$ is used to design a similar adaptation structure to linear multiple-input and multiple-output (MIMO) systems [15]. Next, the PBC control method is applied to the current loop of the CHB converter for grid connection with the model like (10). Adaptive control law can be seen as a feedback control law by adjusting the controller by observing its responses [16]. In the CHB converter, the inductor with inductance L and resistance R is components that always have errors during manufacturing or may not be valued correctly during installation. Therefore, the mathematical model given by (10) is called a system with uncertain parameters, a passivity-based controller like (11) will not have accurate information about the inductor and resistance. On the other hand, the quasi-passive controller (11) depends heavily on the parameters L and R . Here, considering (10), the linear control model with uncertain parameters as a problem of nonlinear systems and applying adaptive control tools to nonlinear systems [15]. Apply the passivity-based controller as presented in [3] assuming that the parameters \hat{R} , \hat{L} , which are the estimated values of R and L respectively, are used to update the passivity-based controller parameters, we have (11):

$$\begin{cases} v_d = \hat{R} i_d^* - \omega \hat{L} i_q^* - r_{1s} (i_d - i_d^*) i_d + v_{sd} \\ v_q = \hat{R} i_q^* + \omega \hat{L} i_d^* - r_{1s} (i_q - i_q^*) i_q + v_{sq} \end{cases} \quad (11)$$

From the kinetic model (10), we have (12):

$$\begin{cases} v_d - v_{sd} = L \frac{di_d}{dt} + R i_d - \omega L i_q \\ v_q - v_{sq} = L \frac{di_q}{dt} + R i_q + \omega L i_d \end{cases} \quad (12)$$

In (12), L and R are the inductor's inductance and resistance values. Set $\tilde{i}_d = i_d^* - i_d$; $\tilde{i}_q = i_q^* - i_q$ as the difference between the set value and the actual value of the current on the two axes dq and $\tilde{L} = L - \hat{L}$; $\tilde{R} = R - \hat{R}$ as the difference between the actual value and the estimated value. With the assumption that the DC voltage control loop and the external power control loops are slow enough compared to the current control loop, then the $\frac{di_d^*}{dt} = \frac{di_q^*}{dt} \approx 0$ values are replaced by (11) and (12), we have (13):

$$\begin{cases} \frac{d\tilde{i}_d}{dt} = -\frac{di_d}{dt} = \frac{\tilde{R}}{L}i_d^* - \omega\frac{\tilde{L}}{L}i_q^* - \left(\frac{r_{1s}}{L} + \frac{R}{L}\right)\tilde{i}_d + \omega\tilde{i}_q \\ \frac{d\tilde{i}_q}{dt} = -\frac{di_q}{dt} = \omega\frac{\tilde{L}}{L}i_d^* + \frac{\tilde{R}}{L}i_q^* - \omega\tilde{i}_d - \left(\frac{r_{2s}}{L} + \frac{R}{L}\right)\tilde{i}_q \end{cases} \quad (13)$$

$$\text{Set } z_1 = \tilde{i}_d = i_d^* - i_d; z_2 = \tilde{i}_q = i_q^* - i_q; \tilde{\theta}_1 = \frac{\tilde{L}}{L}; \tilde{\theta}_2 = \frac{\tilde{R}}{L}$$

Substituting into (13), (14) is written:

$$\begin{bmatrix} \dot{z}_1 \\ \dot{z}_2 \end{bmatrix} = \underbrace{\begin{bmatrix} -\frac{r_{1s}+R}{L} & \omega \\ -\omega & -\frac{r_{2s}+R}{L} \end{bmatrix}}_{\psi} \begin{bmatrix} z_1 \\ z_2 \end{bmatrix} + \underbrace{\begin{bmatrix} -\omega i_q^* & i_d^* \\ \omega i_d^* & i_q^* \end{bmatrix}}_{\Gamma^T} \begin{bmatrix} \tilde{\theta}_1 \\ \tilde{\theta}_2 \end{bmatrix} \quad (14)$$

Equation (14) in matrix form:

$$\dot{\underline{z}} = \underline{\psi}\underline{z} + \Gamma^T\underline{\theta} \quad (15)$$

The control goal is to change the parameters θ_1, θ_2 of the controller so that:

$$\underline{z} \frac{dz}{dt} < 0$$

Determine the valid function V :

$$V(\underline{z}, \underline{\theta}) = \underline{z}^T H \underline{z} + \underline{\theta}^T \Lambda^{-1} \underline{\theta} \quad (16)$$

where $\Lambda \in \mathbb{R}^{2 \times 2}$ is a positive definite symmetric matrix, and $H \in \mathbb{R}^{2 \times 2}$ is also a positive definite symmetric matrix satisfying:

$$\psi^T P + P \psi = -K \quad (17)$$

where $K \in \mathbb{R}^{2 \times 2}$ is a symmetric matrix, positive definite. It is easy to see that the matrix ψ is a stable matrix (with all eigenvalues on the left of the imaginary axis). This ensures that for matrix K , there exists only a symmetric, positive definite matrix H that satisfies (17) [4]. Applying Lyapunov theory to ensure a stable equilibrium $\underline{z} = 0$ requires finding $\underline{\theta}$ such that the derivative $V(\underline{z}) < 0$ along the skewed kinematic trajectory (14). Differentiating (16) along the deviation kinematic trajectory (14), we have (18):

$$\dot{V} = \frac{\partial V}{\partial z} \cdot \frac{dz}{dt} = \tilde{x}^T (\psi^T H + H \psi) \tilde{x} + 2 \tilde{x}^T H \Gamma^T \tilde{\theta} + 2 \Lambda^{-1} \tilde{\theta} \dot{\tilde{\theta}} \quad (18)$$

From here we have the parameter adjustment rule is described in (19):

$$\dot{\tilde{\theta}} = -\Lambda \Gamma H z \quad (19)$$

Substituting (19) into (18) we have (20):

$$\dot{V} = -z^T K z \leq 0 \quad (20)$$

Equation (20) shows that if you choose the parameter adjustment law like (19), the system is guaranteed to be stable in the asymptotic region. To simplify the parameter updating algorithm, we choose P and Λ as diagonal matrices:

$$P = \begin{bmatrix} p_1 & 0 \\ 0 & p_2 \end{bmatrix}, \Lambda = \begin{bmatrix} \lambda_1 & 0 \\ 0 & \lambda_2 \end{bmatrix} \quad (21)$$

In which $p_i, \lambda_i > 0, i = 1, 2$. From there the parameter update rule:

$$\begin{cases} \dot{\tilde{\theta}}_1 = -\lambda_1(-p_1\omega i_q^* z_1 + p_2\omega i_d^* z_2) \\ \dot{\tilde{\theta}}_2 = -\lambda_2(-p_1 i_d^* z_1 + p_2 i_q^* z_2) \end{cases} \quad (22)$$

From (22) we have (23):

$$\begin{cases} \dot{\hat{\theta}}_1 = -\tilde{\theta}_1 = \lambda_1(-p_1\omega i_q^* z_1 + p_2\omega i_d^* z_2) \\ \dot{\hat{\theta}}_2 = -\tilde{\theta}_2 = \lambda_2(-p_1 i_d^* z_1 + p_2 i_q^* z_2) \end{cases} \quad (23)$$

and we have the correction law like (24):

$$\begin{cases} \dot{\hat{L}} = L\lambda_1(-p_1\omega i_q^* z_1 + p_2\omega i_d^* z_2) \\ \dot{\hat{R}} = L\lambda_2(-p_1 i_d^* z_1 + p_2 i_q^* z_2) \end{cases} \quad (24)$$

The parameters p_1, p_2 are chosen based on (17), we choose the matrix K :

$$K = \begin{bmatrix} L & 0 \\ 0 & L \end{bmatrix} \quad (25)$$

Then (8) becomes:

$$\psi^T H + H\psi = \begin{bmatrix} -2p_1 \frac{r_1+R}{L} & (p_1 - p_2)\omega \\ (p_1 - p_2)\omega & -2p_2 \frac{r_2+R}{L} \end{bmatrix} = -K \quad (26)$$

Choosing the parameter $r_1 = r_2 = r$ from (26), the matrix parameter P is chosen as (27).

$$p_1 = p_2 = \frac{L^2}{2(R+r)} \quad (27)$$

Substituting (27) into (24), (28) is written:

$$\begin{cases} \dot{\hat{L}} = \lambda_1 \omega \frac{L^3}{(R+r)} (-i_q^* z_1 + i_d^* z_2) \\ \dot{\hat{R}} = \lambda_2 \frac{L^3}{(R+r)} (i_d^* z_1 + i_q^* z_2) \end{cases} \quad (28)$$

With the parameters λ_1, λ_2 are the adaptive constants when designing the parametric tuner.

The controller for the CHB converter to grid connection must ensure the ability to control active power as well as the ability to receive and generate reactive power independently. The flow controller is a passivity-based adaptive controller and has the structure as shown. The active power controller generates a set value for the d-axis current while the reactive power controller output generates a set value for the q-axis current, both power controllers use a regular PI. So essentially there is only a current loop without an intermediate DC voltage loop, so applying passivity-based to the current loop is very suitable. The current controller on both dq axes is a passivity-based adaptive controller calculated according to formula (2) and parameter adjustment law (19). The overall structure of the CHB converter for grid connection with the passivity-based control method to control the current and voltage of the CHB in the dq coordinate system is shown in Figure 2. The current loop in Figure 2 will help the system control the current, eliminate resonance fluctuations and protect against overcurrent incidents.

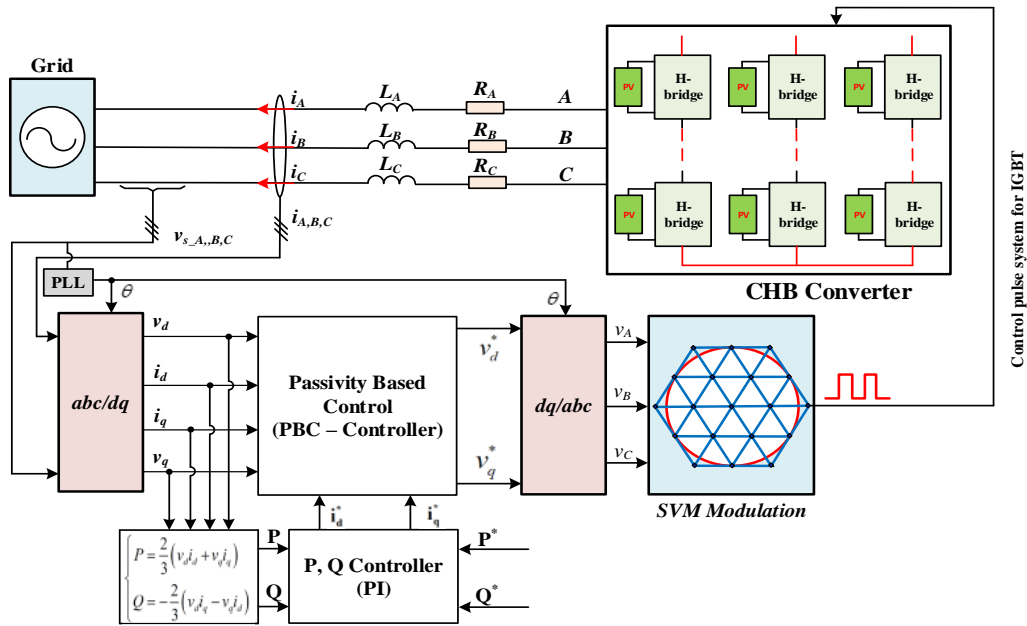


Figure 2. Control system structure for CHB converter

4. RESULTS SIMULATION AND EVALUATION

The simulation parameters for the CHB converter shown in Figures 1 and 2 are presented in Table 1. The simulation results of output voltage v_{NO} are shown in Figure 3. The voltage on three phases v_{NO} of the converter has a 7-level form. The voltage levels are stable, with no transient phenomena at each level of the working process. Figure 4 and Figure 5 are the simulation results of the voltage and current on the AC side load of the CHB converter. The results show that the current and voltage have a standard sinusoidal form, the current reaches a standard sinusoid within the evaluated time period, the amplitude of the current remains stable with a constant value throughout the working process. The resulting voltage has a standard and stable sinusoidal shape. When operating stably, no transient phenomenon occurs.

Table 1. System simulation parameters

Parameter	Value	Parameter	Value
V_{DC}	4,000 V	AC output voltage	3,200 V
Inductance L	4.7 mH	Grid frequency	50 Hz
Resistor R	0.1 Ω	Sampling cycle T_s	200 μ s

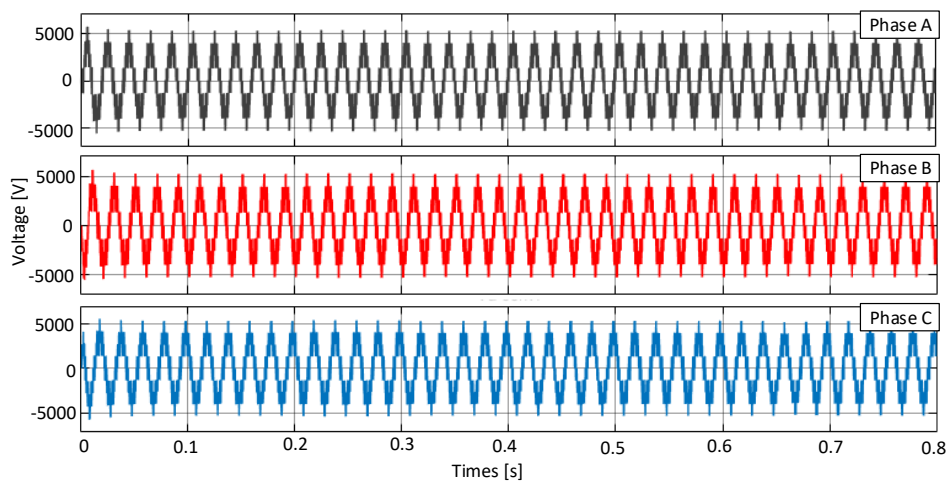


Figure 3. Output voltage on three phases of CHB converter

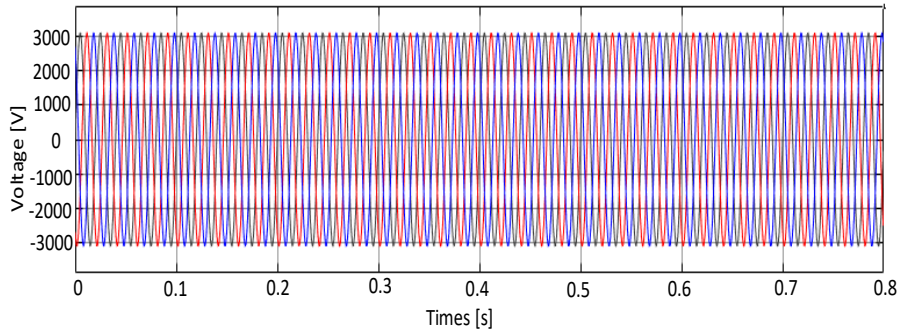


Figure 4. Output voltage on the AC grid side

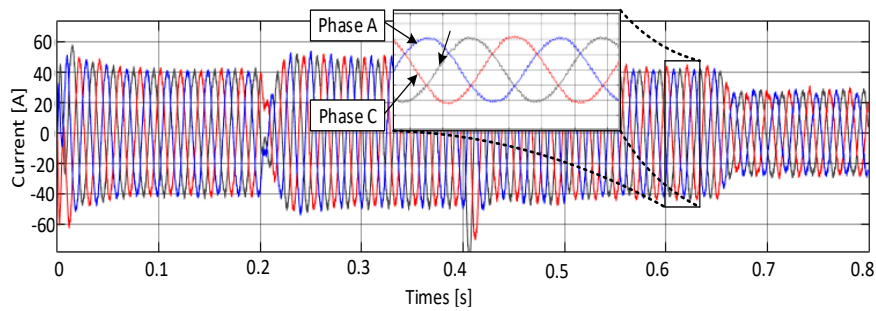


Figure 5. AC grid side current of CHB converter

The results of total harmonic distortion (THD) analysis in Figure 6 and Figure 7 for AC side current and voltage are 0.03% and 4.26% respectively, the high-order harmonics waves with large amplitudes rarely appear, which proves the advantages of applying the passivity-based control method combined with the proposed SVM modulation for the CHB converter. Figure 8 is the shape of the average voltage on the capacitors of phases A, B, C. The results show that during the initial operation of the CHB in the period from 0 to 0.509 s, the capacitor voltage during operation was not stable so there is a transient phenomenon with the highest value being 439 V. When operating stably, the capacitor voltage always fluctuates around the rated value of 400 V. When changing the rated value of the capacitor voltage at a time interval of 0.2 to 0.3 s. The controller always acts so that the capacitor sticks to its set value within a short time of 0.015 s.

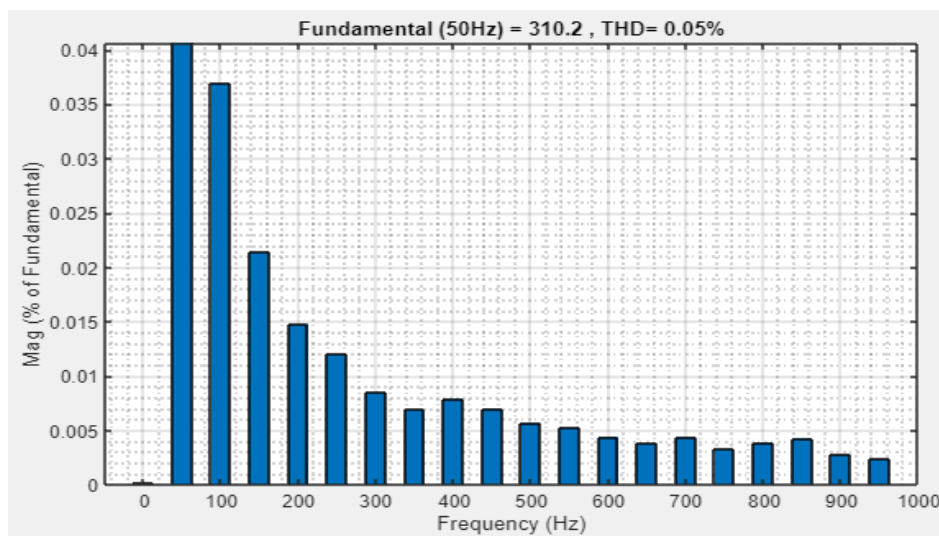


Figure 6. Fourier analysis results of grid-connected AC voltage

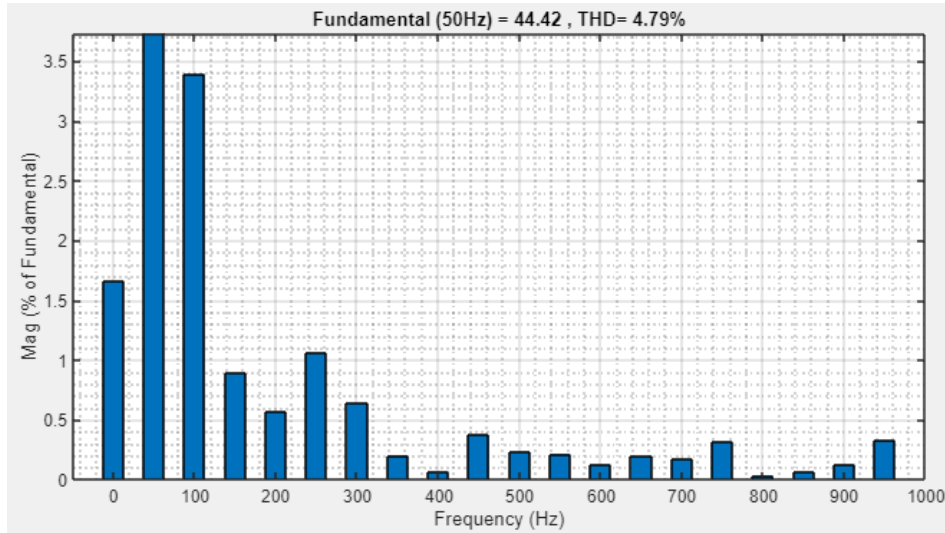


Figure 7. Fourier analysis results of grid-connected AC current

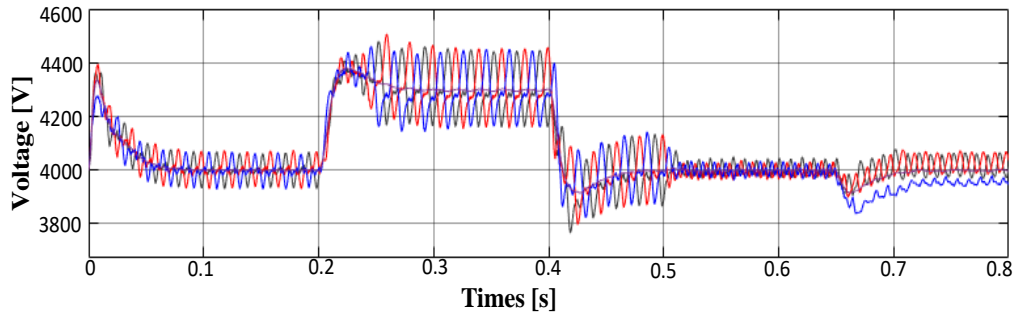


Figure 8. Average voltage across capacitors of phases A, B, C

Figure 9 and Figure 10 are the values of current i_d and current i_q in the dq coordinate system of the converter. The results show that the current i_d and current i_q closely follow the set value with a small fluctuation amplitude. The operating process is stable throughout the period of operation. When changing the set value of current i_d and current i_q , the actual value is also responded quickly due to the timely action of the control algorithm. This proves that the control algorithm combined with the proposed SVM modulation method is reasonable and gives good results in scenarios of changing some set values as well as the working mode of the converter.

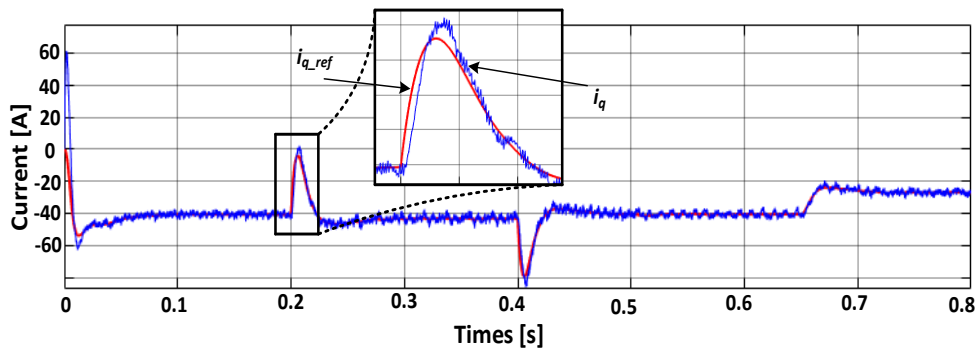


Figure 9. Current i_d in dq coordinate system

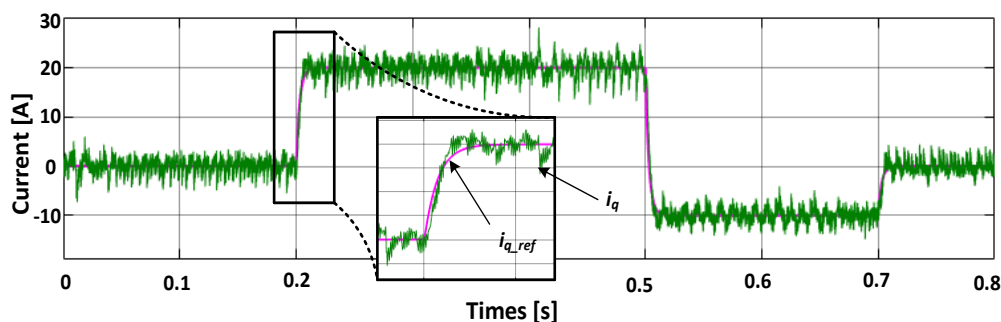


Figure 10. Current i_q in dq coordinate system

5. CONCLUSION

The article has proposed the PV system connects to the grid through the CHB multi-level converter. The conversion process is performed by the SVM modulation method with the rule of expanding the number of unlimited levels for the CHB converter. This modulation method makes the rule expansion process simple while still reducing the number of computational states in the converter. In addition, the voltage balancing process on DC capacitors is performed effectively by taking advantage of the residual states of the modulation process, helping to improve efficiency and reduce complex control design. This is an outstanding advantage of the proposed control method when applied to CHB converters compared with other methods. The grid connection control of the system in the article is performed using the passivity controller, a new control method that requires information from the converter model, then converted to the dq coordinate system to perform control based on pre-established models. This method applies to CHB converters, providing high efficiency. However, this method requires constant parameter updates from the converter to implement the control method. Simulation results have verified the effectiveness of the proposed modulation and control methods.





REFERENCES

- [1] P. K. Achanta, B. B. Johnson, G.-S. Seo, and D. Maksimovic, "A multilevel DC to three-phase AC architecture for photovoltaic power plants," *IEEE Transactions on Energy Conversion*, vol. 34, no. 1, pp. 181–190, Mar. 2019, doi: 10.1109/tec.2018.2877151.
- [2] E. E. Hassan, L. L. Chung, M. F. Sulaima, N. Bahaman, and A. F. A. Kadir, "Smart irrigation system with photovoltaic supply," *Bulletin of Electrical Engineering and Informatics (BEEI)*, vol. 11, no. 1, pp. 29–41, Feb. 2022, doi: 10.11591/eei.v11i1.3338.
- [3] T. Hamdi, K. Elleuch, H. Abid, and A. Toumi, "Sliding mode controller with fuzzy supervisor for MPPT of photovoltaic pumping system," *International Journal of Power Electronics and Drive Systems (IJPEDS)*, vol. 14, no. 3, pp. 1639–1650, Sep. 2023, doi: 10.11591/ijpeds.v14.i3.pp1639-1650.
- [4] H. Jafarian, R. Cox, J. H. Enslin, S. Bhowmik, and B. Parkhideh, "Decentralized active and reactive power control for an AC-stacked PV inverter with single member phase compensation," *IEEE Transactions on Industry Applications*, vol. 54, no. 1, pp. 345–355, Jan. 2018, doi: 10.1109/tia.2017.2761831.
- [5] N. S. M. Taib, S. Z. M. Noor, S. Musa, and P. D. A. Aziz, "Fuzzy logic control based MPPT for standalone photovoltaic system with battery storage," *International Journal of Power Electronics and Drive Systems (IJPEDS)*, vol. 14, no. 4, pp. 2527–2536, Dec. 2023, doi: 10.11591/ijpeds.v14.i4.pp2527-2536.
- [6] B. V. Rajanna and M. K. Kumar, "Comparison study of lead-acid and lithium-ion batteries for solar photovoltaic applications," *International Journal of Power Electronics and Drive Systems (IJPEDS)*, vol. 12, no. 2, pp. 1069–1082, Jun. 2021, doi: 10.11591/ijpeds.v12.i2.pp1069-1082.
- [7] N. Mezzai, S. Belaid, D. Rekioua, and T. Rekioua, "Optimization, design and control of a photovoltaic/wind turbine/battery system in Mediterranean climate conditions," *Bulletin of Electrical Engineering and Informatics (BEEI)*, vol. 11, no. 5, pp. 2938–2948, Oct. 2022, doi: 10.11591/eei.v11i5.3872.
- [8] X. Hou, Y. Sun, H. Han, Z. Liu, W. Yuan, and M. Su, "A fully decentralized control of grid-connected cascaded inverters," *IEEE Transactions on Sustainable Energy*, vol. 10, no. 1, pp. 315–317, Jan. 2019, doi: 10.1109/tpwr.2018.2816813.
- [9] M. Lu, S. Dutta, V. Purba, S. Dhople, and B. Johnson, "A grid-compatible virtual oscillator controller: analysis and design," *2019 IEEE Energy Conversion Congress and Exposition (ECCE)*, Baltimore, MD, USA, 2019, pp. 2643–2649, doi: 10.1109/ecce.2019.8913128.
- [10] S. S. Katkamwar and V. R. Doifode, "Cascaded H-bridge multilevel PV inverter with MPPT for grid connected application," *2016 International Conference on Energy Efficient Technologies for Sustainability (ICEETS)*, Nagercoil, India, 2016, pp. 641–646, doi: 10.1109/iceets.2016.7583832.
- [11] M. E. Ahmad, A. H. Numan, and D. Y. Mahmood, "Enhancing performance of grid-connected photovoltaic systems based on three-phase five-level cascaded inverter," *International Journal of Power Electronics and Drive Systems (IJPEDS)*, vol. 12, no. 4, pp. 2295–2304, Dec. 2021, doi: 10.11591/ijpeds.v12.i4.pp2295-2304.
- [12] A. H. Ali, H. S. Hamad, and A. A. Abdulrazzaq, "An adaptable different-levels cascaded H-bridge inverter analysis for PV grid-connected systems," *International Journal of Power Electronics and Drive Systems (IJPEDS)*, vol. 10, no. 2, pp. 831–841, Jun. 2019, doi: 10.11591/ijpeds.v10.i2.pp831-841.
- [13] H. Jafarian, S. Bhowmik, and B. Parkhideh, "Hybrid current-/voltage-mode control scheme for distributed AC-stacked PV inverter with low-bandwidth communication requirements," *IEEE Transactions on Industrial Electronics*, vol. 65, no. 1, pp. 321–330, Jan. 2018, doi: 10.1109/tie.2017.2714129.





- [14] S. Essakiappan, H. S. Krishnamoorthy, P. Enjeti, R. S. Balog, and S. Ahmed, "Multilevel medium-frequency link inverter for utility scale photovoltaic integration," *IEEE Transactions on Power Electronics*, vol. 30, no. 7, pp. 3674–3684, Jul. 2015, doi: 10.1109/tpe.2014.2350978.
- [15] C. Han *et al.*, "Evaluation of cascade-multilevel-converter-based STATCOM for Arc Furnace Flicker mitigation," *IEEE Transactions on Industry Applications*, vol. 43, no. 2, pp. 378–385, 2007, doi: 10.1109/tia.2006.889896.
- [16] M. Rejas *et al.*, "Performance comparison of phase shifted PWM and sorting method for modular multilevel converters," *2015 17th European Conference on Power Electronics and Applications (EPE'15 ECCE-Europe)*, Geneva, Switzerland, 2015, pp. 1-10, doi: 10.1109/epe.2015.7311700.
- [17] A. Dekka, B. Wu, N. R. Zargari, and R. L. Fuentes, "A space-vector PWM-based voltage-balancing approach with reduced current sensors for modular multilevel converter," *IEEE Transactions on Industrial Electronics*, vol. 63, no. 5, pp. 2734–2745, May 2016, doi: 10.1109/tie.2016.2514346.
- [18] M. Coppola *et al.*, "Modulation technique for grid-tied PV multilevel inverter," *2016 International Symposium on Power Electronics, Electrical Drives, Automation and Motion (SPEEDAM)*, Capri, Italy, 2016, pp. 923-928, doi: 10.1109/speedam.2016.7525980.
- [19] J. Pou, J. Zaragoza, S. Ceballos, M. Saeedifard, and D. Boroyevich, "A carrier-based PWM strategy with zero-sequence voltage injection for a three-level neutral-point-clamped converter," *IEEE Transactions on Power Electronics*, vol. 27, no. 2, pp. 642–651, Feb. 2012, doi: 10.1109/tpe.2010.2050783.
- [20] S. Nagar, S. Khan, and B. Singh, "Performance of cascaded diode bridge integrated H-bridge 13 level multilevel inverter," *2017 Recent Developments in Control, Automation & Power Engineering (RDCAPE)*, Noida, India, 2017, pp. 399-403, doi: 10.1109/rdcape.2017.8358304.
- [21] R. Ortega and E. García-Canseco, "Interconnection and damping assignment passivity-based control: a survey," *European Journal of Control*, vol. 10, no. 5, pp. 432–450, Jan. 2004, doi: 10.3166/ejc.10.432-450.
- [22] A. Dell'Aquila, M. Liserre, V. G. Monopoli, and P. Rotondo, "Overview of PI-based solutions for the control of DC buses of a single-phase H-bridge multilevel active rectifier," *IEEE Transactions on Industry Applications*, vol. 44, no. 3, pp. 857–866, 2008, doi: 10.1109/tia.2008.921405.
- [23] H. Miranda, V. Cardenas, G. Espinosa-Perez, and D. Noriega-Pineda, "Multilevel cascade inverter with voltage and current output regulated using a passivity - based controller," *Conference Record of the 2006 IEEE Industry Applications Conference Forty-First IAS Annual Meeting*, Tampa, FL, USA, 2006, pp. 974-981, doi: 10.1109/ias.2006.256643.
- [24] D. Gerardo, E. Palacios, and V. Cardenas, "Interconnection and damping passivity-based control applied to a single-phase voltage source inverter," *12th IEEE International Power Electronics Congress*, San Luis Potosi, Mexico, 2010, pp. 229-234, doi: 10.1109/ciep.2010.5598907.
- [25] G. Sandoval, H. Miranda, G. Espinosa-Pérez, and V. Cárdenas, "Passivity-based control of an asymmetric nine-level inverter for harmonic current mitigation," *IET Power Electronics*, vol. 5, no. 2, p. 237, 2012, doi: 10.1049/iet-pel.2010.0131.
- [26] A. Donaire, R. Ortega, and J. G. Romero, "Simultaneous interconnection and damping assignment passivity-based control of mechanical systems using generalized forces," *Arxiv.org/abs/1506.07679*, Jun. 2015.

BIOGRAPHIES OF AUTHORS



Tran Hung Cuong     received his engineer (2010), MSc (2013) degrees in industrial automation engineering from Hanoi University of Science and Technology and completed PhD degree in 2020 from Hanoi University of Science (HUST). Now, he is a lecturer of Faculty of Electrical and Electronic Engineering under Thuy Loi University (TLU). His current interests include power electronic converters, electric motor drive, convert electricity from renewable energy sources to the grid, saving energy solutions applied for grid and transportation. He can be contacted at email: cuongth@utc.edu.vn.



An Thi Hoai Thu Anh     received her engineer (1997), MSc (2002) degrees in industrial automation engineering from Hanoi University of Science and Technology, and completed PhD degree in 2020 from University of Transport and Communications (UTC). Now, she is a lecturer of Faculty of Electrical and Electronic Engineering under University of Transport and Communications (UTC). Her current interests include power electronic converters, electric motor drive, saving energy solutions applied for industry and transportation. She can be contacted at email: htanh.ktd@utc.edu.vn.